Title
Microwave Synthesis of Colloidal Germanium Nanoparticles

Author
Lundervold, Jesse

Publication Date
2021

Peer reviewed|Thesis/dissertation

Microwave Synthesis of Colloidal Germanium Nanoparticles

By

JESSE LUNDERVOLD
THESIS

Submitted in partial satisfaction of the requirements for the degree of

MASTER OF SCIENCE

in

CHEMISTRY

in the

OFFICE OF GRADUATE STUDIES

of the

UNIVERSITY OF CALIFORNIA

DAVIS

Approved:

Susan M. Kauzlarich, Chair

Jesús Velázquez

Marie Heffern

Committee in Charge

2021

Acknowledgements

I would like to thank my advisor Dr. Susan Kauzlarich for all of her support and guidance while I've been both an REU student and as a graduate student in her lab. I would also like to thank my lab mates, past and present who have offered their guidance and friendship: Dr. Kathryn Newton, Dr. Katayoun Tabatabei, Dr. Kasey Devlin, Dr. Chrisopher Perez, Xiao Qi, Zheng Ju, Allan He, Andy Justl, Ashlee Hauble, Tanner Kimberly. I am very grateful to Dr. Kathryn Newton for being a fantastic mentor during my REU experience at UCD and allowing me to work with her on her projects. Thank you to Emily Tseng for allowing me to aid in your undergraduate research. I know you're destined for big things.

A huge thank you to Amanda Bohanon, Sarah Dishman, and Lilia Baldauf for being some of the most supportive and kind people I have had the pleasure of calling my friends. A thank you to my friends who have supported me from across the country: Trevor Nicks, Brianna Steiert, Seki Anderson, and Alexandra Millhuff, and to Lex, Jenna, and the entirety of our friend group for adding so much levity to my life the past two years.

Lastly, thank you to my mom for always being there for me and to my cat, Hildegard who helped immensely in the writing process for this thesis.

ABSTRACT

Microwave Synthesis of Colloidal Germanium Nanoparticles

Group IV elements, such as silicon and germanium, have been of much of interest due to their semi-conducting properties on the nanoscale. On the nanoscale, quantum confinement effects result in changes in electronic and optic properties than can be tuned through altering synthesis methods. Germanium nanoparticles (Ge NPs) have been investigated for their potential use in a wide variety of areas including for energy conversion, biological imaging, and in optoelectronics. Ge NPs experience quantum confinement when synthesized to < 24 nm in diameter, allowing quantum confinement effects to be seen at relatively large NP size and tuned through changes in NP size. The surface ligand of NPs as well as the NP shape are other ways in which electronic properties of semi-conducting NPs can be altered. The goal of this research is to synthesize and characterize the properties of Ge NPs with varying sizes, surface ligands, and shape.

This thesis presents synthesis methods and the characterization of Ge NPs with varying surface ligands and of Ge NPs synthesized using a known shape-directing agent. The results of these experiments are described in two chapters: (1) Extinction Coefficient of Germanium Nanoparticles, (2) Shape Control of Germanium Nanoparticles with Polyvinylpyrrolidone.

TABLE OF CONTENTS

LIST OF FIGURES

LIST OF TABLES

CHAPTER 1

Introduction

Germanium is an indirect band semi-conductor with a band gap 0.67 eV in the bulk phase.[1] The Bohr radius of Ge (<24 nm) allows quantum confinement properties to be seen across of range of Ge NP sizes. The tunability of optical properties based on size and the low toxicity of Ge nanoparticles (Ge NPs) make them applicable in a wide variety of fields including biological imaging, optoelectronics, and batteries.[2,3,4] Solution synthesis of Ge NPs is also varied, with germanium halides, germanium oxides, and organo-germanium compounds utilized as Ge precursors in the presence of strong reducing agents such as lithium aluminum hydride and lithium borohydride.[2] Sol-gel, decomposition, and microwave-assisted synthesis routes have also been successful in producing Ge NPs.[2,5]

The tunability of optical properties can be further influenced by the surface ligand, shape, and size of NPs. The surface ligand can help to control the shape of NPs while also preventing oxidation and agglomeration of NPs.[3,6] Ge NPs can also readily undergo ligand exchanges following initial synthesis.[7] Ligand exchanges can further increase stability of Ge NPs and aid in the subsequent use of Ge NPs in thin films.[5,7] Through altering synthesis conditions, Ge NPs of different shapes can also be observed. Reported shapes of Ge NPs include spherical Ge NPs, Ge NP cubes, and tetrahedra.[8] Similarly, the size of Ge NPs can be modified through a ratio of precursors or through a change in reducing agent.[4,5,8]

This thesis explores the microwave-assisted synthesis of Ge NPs and the effects of synthetic parameters on size and shape of Ge NPs. The synthesis of NPs with tunable shapes and sizes and the effect this has on NP properties is an area that continues to be studied. The

subsequent chapters describe the investigation of Ge NP synthesis as it pertains to synthesis parameters effecting size, shape, and optical properties.

CHAPTER 2

Extinction Coefficient of Germanium Nanoparticles

INTRODUCTION

Microwave-assisted heating in nanoparticle (NP) synthesis is a relatively recent area of research and has shown promising results. Methods of microwave-heating have the advantages of shorter reaction times, energy efficiency, and the potential for reaction scale-up when compared to conventional heating.[9] Microwave heating also uniformly heats the solution, with the hottest temperature being localized in the reaction instead of on the walls of the vessel as with conventional heating.[9] This inverse heating gradient allows for constant temperature distribution and the direct heating of any microwave absorbers in the reaction.[9,10] Colloidal NPs, noble metal NPs, semiconducting NPs, carbon nanostructures, and more have been successfully synthesized using this method.[11]

Nanoscale germanium has been synthesized colloidally in many ways, including through the use of different germanium precursors and a variety of synthesis methods.[12-8] Previous work has shown that microwave heating of germanium precursors produced more uniform and more crystalline NPs at lower temperatures when compared to conventional heating.[5]

Changing the NP size, shape, and surface ligand can all impact the electronic and optoelectronic properties of the material. For example, changing the size of the NP has been shown to increase the molar extinction coefficient, ε, of semiconducting quantum dots.[13] Knowing the molar extinction coefficient can in turn aid in the determination of solution concentration through the relationship of Beer's Law. For a wide variety of applications, knowing the both the concentration and molar extinction coefficient can be advantageous in exploiting the optical properties of nanomaterials. Extinction coefficients for CdS, CdTe, and

CdSe were determined by Yu et al. and were found to be dependent on the size of the NPs.[14] All three types of NPs showed a direct relationship between size and extinction coefficient. It was also found that the extinction coefficients were not significantly different when the surface ligand, solvent, or synthetic method was changed.[14] Similar trends between size and extinction coefficient have also been found for ZnSe NPs.[15,16]

This chapter outlines the experiments undertaken in order to examine the extinction coefficient of Ge NPs of three different sizes with two different surface ligands. Advancements in the synthesis of nanomaterials allows for the determination of the extinction coefficient of nanomaterials as it pertains to size and surface chemistry. The goal of this experiment is to investigate the effects of size and surface ligand on the extinction coefficient of Ge NPs.

EXPERIMENTAL

Methods - Germanium Nanoparticle Synthesis:

All samples were prepared in an Ar-filled glovebox. Mole of GeI_2 and GeI_4 (purchased from Dr. Richard Blair's laboratory at the University of Central Florida) ranging from 0.4 to 1.5 were added to a 35-mL microwave tube with 8 mL of degassed oleylamine (Sigma-Aldrich, >98%). Oleylamine (OAM) was degassed on the Schlenk line. The sample was sealed with a cap inside the glove box and parafilmed three times after being taken out. After dissolving the germanium precursors via sonication, the sample was yellow in color. It was then heated for 30 minutes at 250°C in a CEM microwave reactor. The color of the sample changed to a dark brown during this heating period, indicating the formation of OAM-capped Ge NPs.

Nanoparticle Isolation:

Microwaved samples were triple-wrapped in parafilm and transferred back into the glove box and the contents were transferred into a centrifuge tube. The catalyst tower was closed before isolating the sample in the glove box to prevent any amine contamination of the catalyst. Approximately 30 mL of anhydrous methanol was added, and the sample was taken out of the glove box and centrifuged at 8500 RPM for 15 minutes. The centrifuge tube was triple wrapped and transferred back into the glove box. The colorless supernatant was discarded and the nanoparticles on the side of the centrifuge tube were resuspended in 5 mL of toluene. Toluene used inside the glove box were purchased from Fisher Scientific and purified using a solvent purification system. All samples (NPs in toluene) were stored in glass screw-top vials within the glove box.

Ligand Substitution:

A 2 mL portion of resuspended NPs in toluene sample was transferred to a centrifuge tube in addition to 1 mL of hydrazine (Sigma-Aldrich, 98%). The centrifuge tube was taken out of the glove box, triple-wrapped with parafilm, and then sonicated for 90 minutes. The addition of acetonitrile and subsequent sonication of the sample strips the OAM ligand from the surface of the NPs. Following sonication, the sample is still homogenous with no color change or layer formation. The NP-acetonitrile sample was then centrifuged for 10 minutes at 8500 RPM. The catalyst tower was closed again and the sample was taken into the glove box and the clear supernatant was discarded. The precipitate was washed with acetonitrile (Fisher Scientific, 98%) and transferred to a 35-mL microwave tube. 6 mL of anhydrous dodecanethiol (DDT) (Sigma Aldrich, 98%) was added to the precipitate in the microwave tube. The sample consisting of bare Ge NPs and DDT was heated at 150°C for one hour in a CEM microwave reactor. The now

DDT-capped Ge NPs were centrifuged for 10 minutes and then resuspended in toluene for storage as done for the OAM-capped Ge NPs.

Powder X-ray Diffraction (PXRD):

OAM and DDT-capped Ge NP suspensions were prepared for PXRD measurements by collecting 0.1 to 0.3 mL of stored sample in a plastic syringe. The syringe was capped and taken out the box. The sample was drop-casted onto a silicon zero-background holder while the holder was heated gently on a hot plate. A Bruker D8 diffractometer (Cu Kα source, λ = 1.5418 Å) was used to collect PXRD data from the 20° to 80° 2θ. The PXRD patterns were compared to diamond cubic Ge (04-0545) diffraction file from the International Center for Diffraction Data.

FT-IR:

Samples of Ge NPs in toluene were deposited directly onto crystal on a Bruker Alpha spectrometer. FT-IR measurements were taken after the sample was allowed to air dry.

NIR-UV-Vis:

1 mL of a capped or recapped sample was taken out of the glove box in a 5 mL glass vial. This sample was then transferred into a quartz cuvette using a micropipette. 2 mL of toluene (Sigma-Aldrich) was dispensed via micropipette to dilute the 1-mL sample of Ge NPs. UV-Vis spectra were collected for serial dilutions of each Ge NP sample. A spectrum of each dilution was collected on a UV-3600 Plus Shimadzu UV-vis-NIR spectrophotometer at room temperature from 1600 to 250 nm. The sampling interval was 1 nm.

Extinction Coefficient:

Beer's Law plots were generated using the absorption at 700 and 800 nm, two wavelengths at the absorption onset in the UV-Vis spectra, and the concentration of Ge for each dilution of each sample. Concentrations of diluted samples were calculated assuming there was 100% conversion of Ge precursors to Ge NPs. The slope of the Beer's Law plot provided the extinction coefficient of the sample.

Tauc Plots:

Tauc plots were created by taking the nth root of the product of the absorbance of the Ge NPs and the energy, $(Ahv)^{\frac{1}{n}}$, vs. the energy in electron volts. For direct transitions, n=1/2 and n=2 for indirect transitions.[17] A tangent line of 1.8 eV to 2.0 eV was extended until it crossed the x-axis; the approximate band-gap of the Ge NPs is the x-intercept of the tangent line.[18]

DISCUSSION/RESULTS:

Figure 2-1 show the PXRD patterns for Ge NPs capped with OAM and following a ligand exchange of OAM to DDT. The pattern of the OAM-capped Ge NPs has five peaks ranging from 20 to 80 degrees, with the two peaks 65 and 72.8 degrees being less prominent. The same peaks can be seen in the pattern of the Ge NP sample recapped with DDT. All the peaks have much lower intensity in the DDT-capped sample with the two peaks at higher 2θ almost not appearing at all. Both diffraction patterns display the five peaks characteristic of diamond cubic Ge (PDF 04-0545) and correspond to Ge (hkl) values. The higher intensity of the OAM-capped Ge NP pattern indicates that there is material loss in the recapping process that leads to lower diffraction intensity and also causing less material deposited onto the sample holder.

PXRD patterns for OAM-capped Ge NPs synthesized with varying amounts of Ge precursors are shown in Figure 2-2. All Ge NPs prepared using different precursor ratios have the same five peaks that are characteristic of diamond cubic Ge. The ratio of 0.28 mmol of GeI_2 to 0.12 mmol GeI_4 produced Ge NPs that had the narrow diffraction peaks compared to Ge NPs synthesized with lesser amounts of GeI_4. There are extra peaks below 20 degrees for both the 0.3:0.1 Ge NPs and the 0.28:0.12 Ge NPs. This is most likely from residual OAM impurities that was not washed out of the sample during the NP isolation procedure.

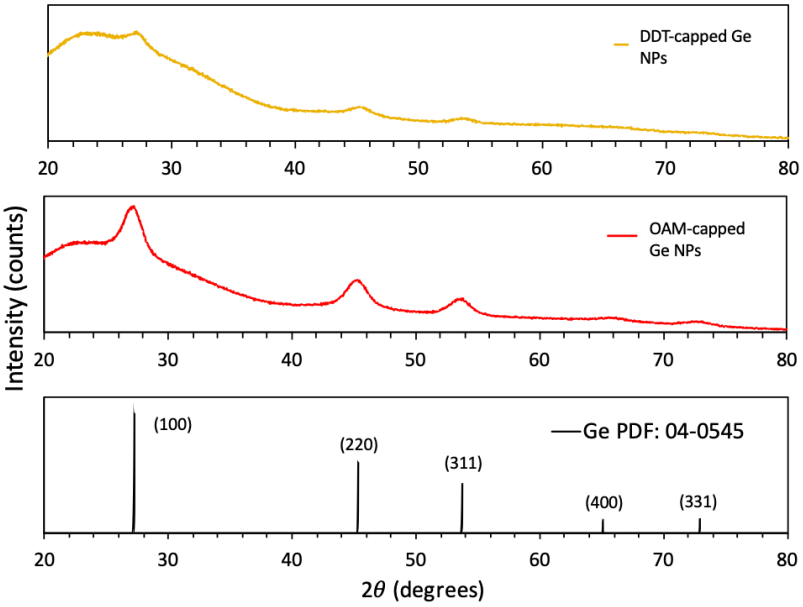

Figure 2-1 PXRD patterns of OAM-capped Ge NPs synthesized with 0.4 mmol GeI_2 in 8 mL OAM and the same sample of Ge NPs following a ligand exchange with DDT (top). Compared to a Ge reference pattern (Ge PDF 04-0545) with corresponding Ge (hkl) values.

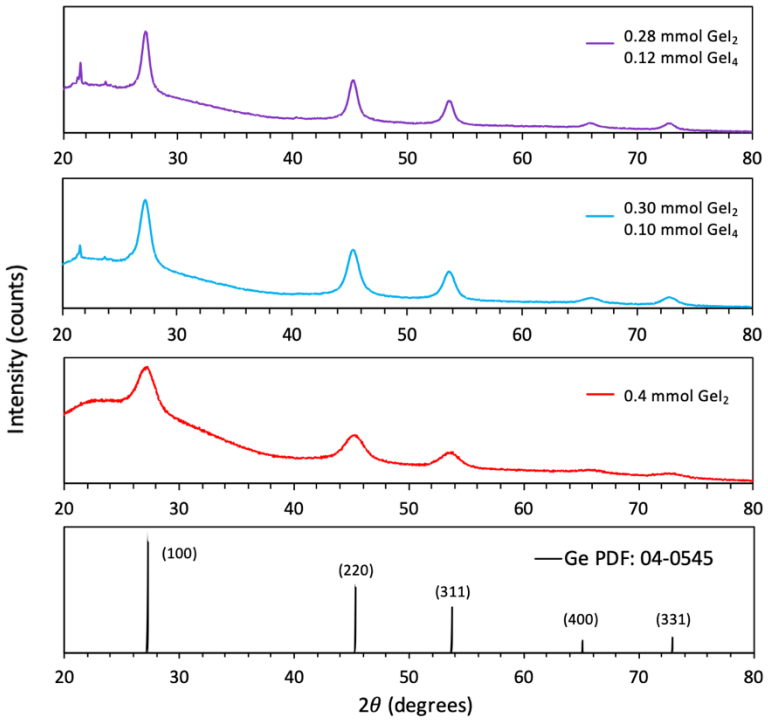

Figure 2-2 Powder X-Ray diffraction patterns of OAM-capped Ge NPs synthesized with varying amounts of GeI_2 (0.4-0.28 mmol GeI_2) and GeI_4 (0-0.12 mmol GeI_4) as compared to Ge reference pattern.

OAM-capped Ge NPs were recapped with DDT and PXRD patterns of Ge NPs prepared with two different ratios of Ge precursors are shown in Figure 2-3. The recapped Ge NPs synthesized with 0.3 mmol of GeI_2 and 0.1 mmol GeI_4 have sharper peaks than the NPs prepared from 0.4 mmol GeI_2. The peaks between 60 and 80 degrees are not distinguishable in the diffraction pattern for this sample of Ge NPs. The two peaks below close to 20 degrees not corresponding to Ge that were present in the OAM-capped sample of 0.3:0.1 Ge NPs are no

longer present after recapping with DDT. This indicates that the residual (?) was washed out during the ligand-exchange procedure.

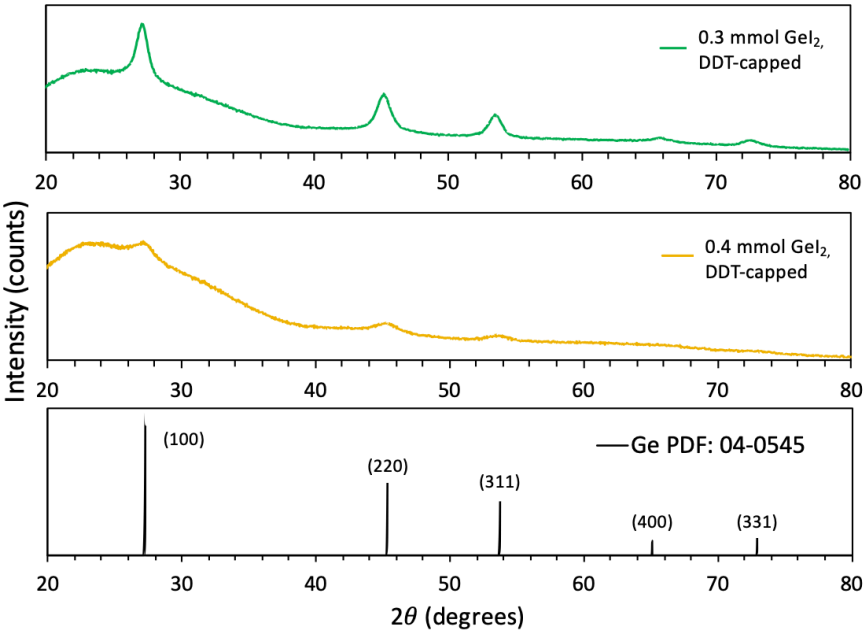

Figure 2-3 PXRD patterns of DDT-capped Ge NPs prepared with 0.4 and 0.3 mmol GeI_2 precursor compared to Ge reference pattern.

Crystallite size of OAM and DDT-capped Ge NPs was obtained through peak fitting of the corresponding PXRD pattern and is shown in Table 2-1. Crystallite size was determined through peak refinement of the (110), (220), and (311) diffraction peaks using JADE software.[19] The largest Ge NPs were around 10 nm and the smallest being close to 4 nm.

Table 2-1 Germanium Precursor Ratio to Crystallite Size of Corresponding Ge NPs

GeI_2:GeI_4	Crystallite size (nm)
0.4:0	4.40 ± 0.06
0.3:0.1	7.21± 0.12
0.28:0.12	9.80 ± 0.04

The IR spectrum of OAM-capped Ge NPs prepared with 0.4 mmol of GeI_2 is is shown in Figure 2-4 in comparison to the same NPs following a ligand exchange. The spectrum of OAM-capped Ge NPs has a small peak at 3002 cm^{-1} and two sharp peaks at 2922 and 2852 cm^{-1}. There are also multiple small peaks around 1500 cm^{-1}. The DDT-capped Ge NP spectra does not feature the small peak at just above 3000 cm^{-1} that was present before the ligand exchange. The peak at ~1500 cm^{-1} is still present after recapping even though the other smaller peaks around 1500 cm^{-1} are not.

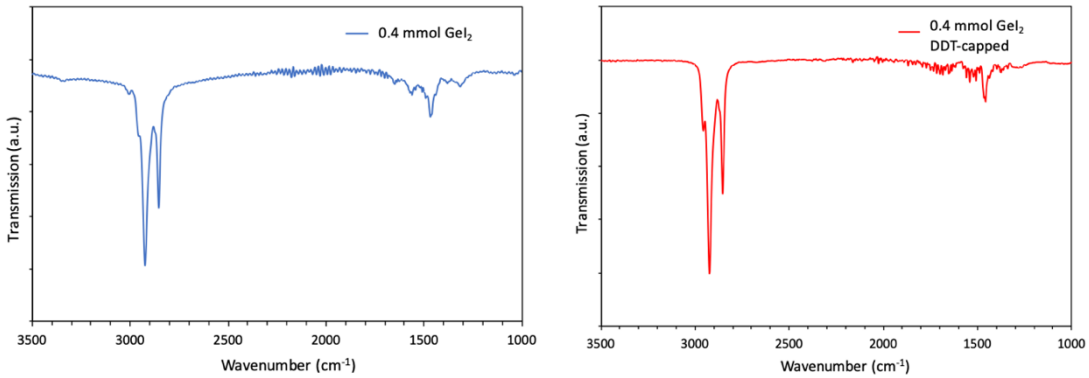

Figure 2-4 FTIR spectra of OAM-capped Ge NPs (left) and the same Ge NPs with exchanged DDT ligand (right).

Figure 2-5 shows the FT-IR spectra of OAM- and DDT-capped Ge NPs prepared with varying amounts of Ge precursor. The spectra of both the 0.3:0.1 and 0.28:0.12 OAM-capped Ge NPs display similar peaks to the 0.4:0 OAM-capped Ge NPs. The DDT-capped Ge NPs also both do not have the small peak at 3000 cm^{-1} present in the OAM-capped Ge NPs spectra.

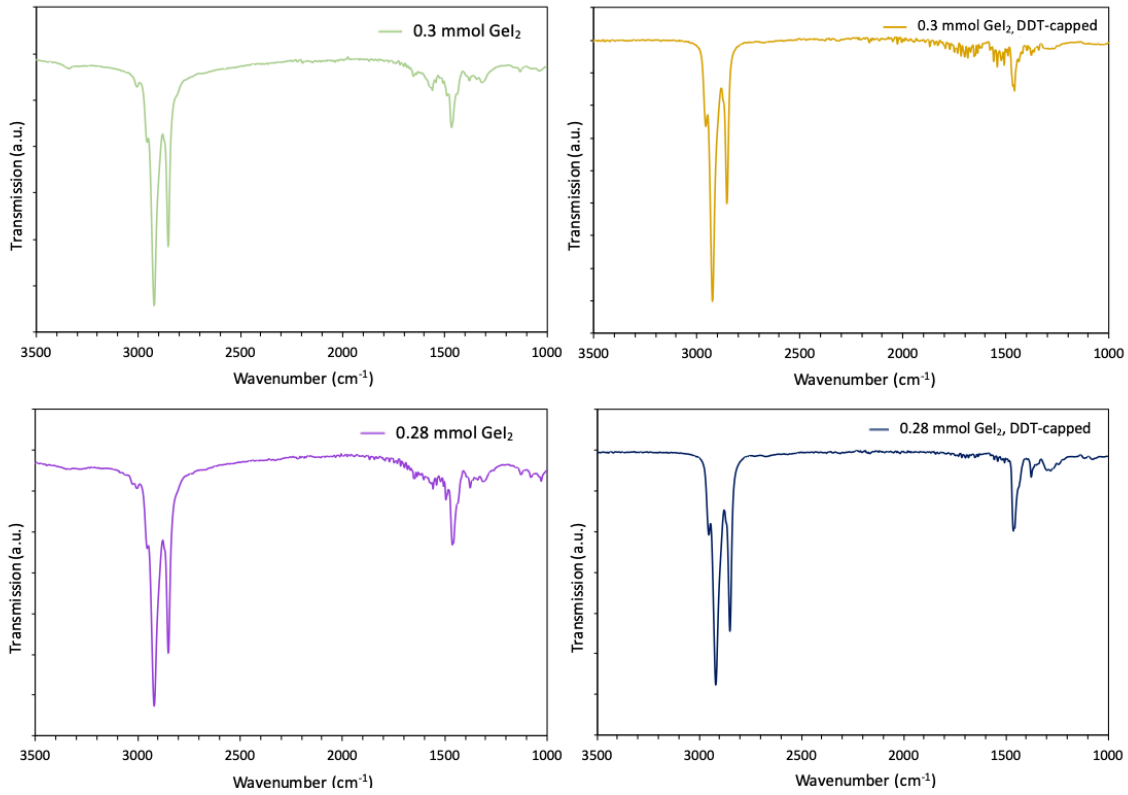

Figure 2-5 FT-IR spectra of OAM-capped Ge NPs with 0.28 and 0.3 mmol GeI_2 precursor and the same samples after ligand exchange with DDT.

A 1-mL sample of OAM-capped Ge NPs was taken out of the glovebox and with toluene to collect absorbance spectra. Figure 2-6 is the spectra obtained from the serial dilutions collected from 0.4:0 OAM-capped Ge NPs with corresponding Ge concentrations. Concentrations were calculated assuming there is a 100% conversion of Ge precursors to NPs. Absorption spectra of 0.3:0.1 and 0.28:0.12 OAM- and DDT-capped Ge NPs are shown in Figure 2-7. The peaks at 900 and 947 nm and the set of peaks between 1100 and 1200 nm are the cause of residual OAM in the sample. The absorption values from 700 nm and 800 nm for each dilution in conjunction with the Ge concentrations were used to generate a Beer's Law plot (Figure 2-9).

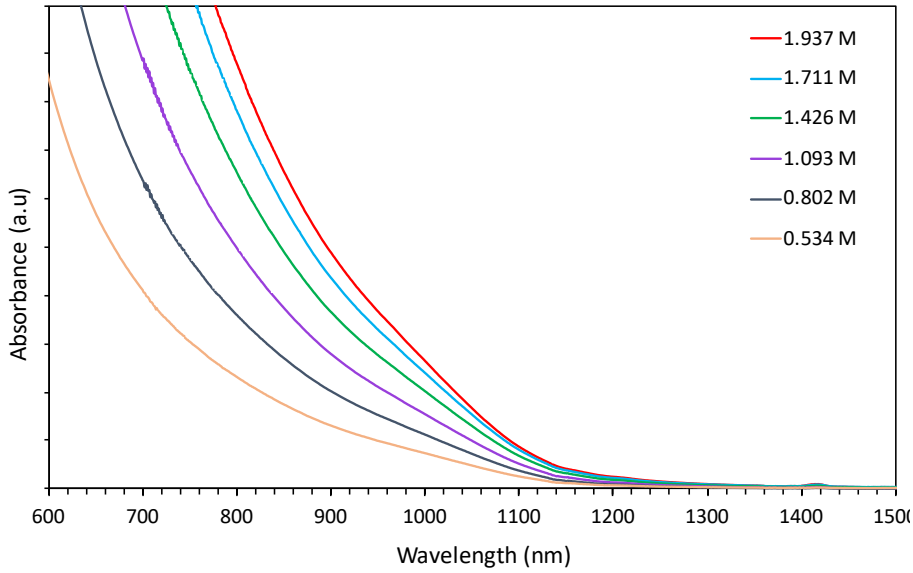

Figure 2-6 Absorption spectra of serial dilutions of 0.4:0 OAM-capped Ge NPs.

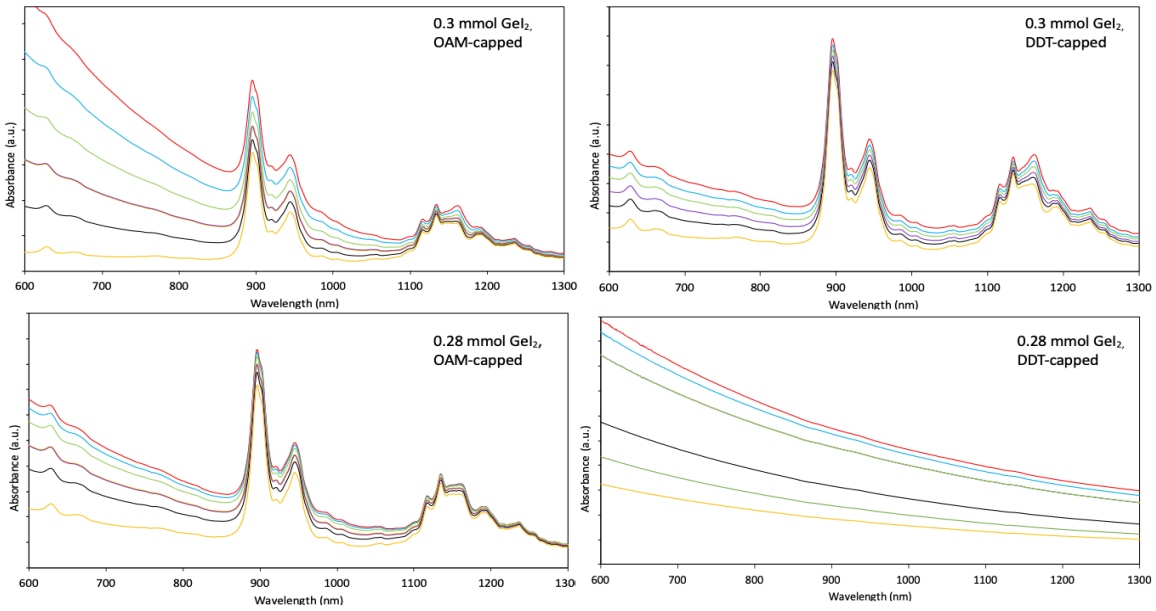

Figure 2-7 Spectra of serial dilutions of OAM-capped Ge NPs with 0.28 and 0.3 mmol GeI_2 precursor and the same samples after ligand exchange with DDT.

A Beer's Law plot is the relationship between the concentration vs. absorption of a solution with the slope of the data being the extinction coefficient, or molar absorptivity, of the

solution. The concentrations calculated for the serial dilutions and the corresponding absorbance values were used to create Beer's Law plots for each OAM-capped sample. Shown below is the Beer's Law plot for the 4 nm OAM-capped Ge NPs.

The extinction coefficient should not change once the ligand is exchanged but would change with the size of the NP. Comparison of extinction coefficients for the three sizes of synthesized Ge NPs is shown below in Table 2-2.

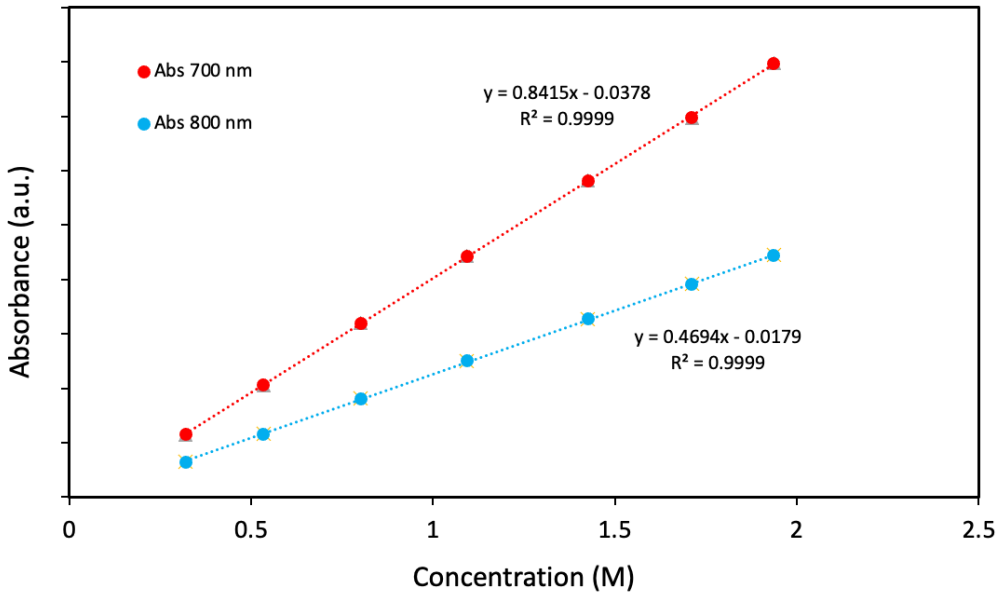

Figure 2-8 Beer's Law plot of 0.4:0 OAM-capped Ge NPs at 700 and 800 nm.

The extinction coefficient should not change once the ligand is exchanged but would change with the size of the NP. Comparison of extinction coefficients for the three sizes of synthesized Ge NPs is shown below in Table 2-2.

Table 2-2 Extinction Coefficients at 700 and 800 nm For Three Different Sizes of Ge NPs

Sample	Extinction coefficient at 700 nm (M^{-1} cm^{-1})	Extinction coefficient at 800 nm (M^{-1} cm^{-1})
0.4:0 Ge NPs (OAM and DDT-capped)	0.842 ± 0.003	0.469 ± 0.002
0.3:0.1 Ge NPs (OAM and DDT-capped)	2.916 ± 0.019	1.336 ± 0.018
0.28:0.12 Ge NPs (OAM and DDT-capped)	1.019 ± 0.008	0.640 ± 0.006

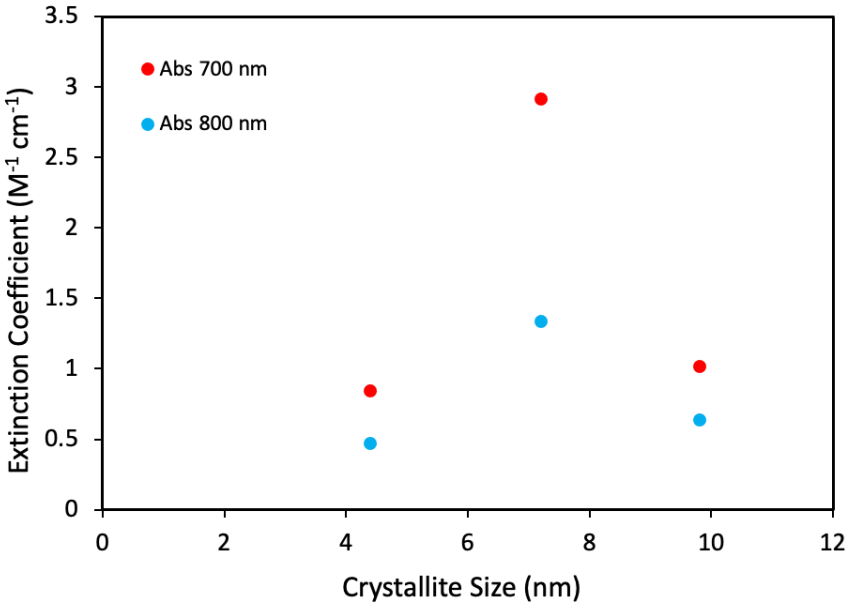

Figure 2-9 The extinction coefficient of Ge NPs at 700 and 800 nm as a function of crystallite size.

The band gap of each of the Ge NPs was determined via Tauc plot (Figure 2-5). The band gap decreases with increasing Ge NP size, with the band gap of the 7 and 10 nm NPs being very close together, as shown in Table 2-3.

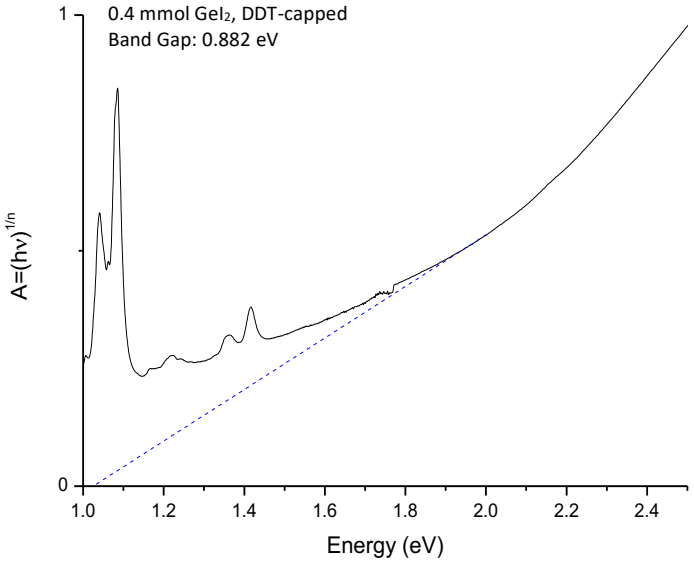

Figure 2-10 Tauc plot for DDT-capped Ge NPs prepared with 0.4 mmol GeI_2 with tangent line added.

Table 2-3 Band Gap Energies for Three Sizes of OAM-capped Ge NPs

Sample	Band gap (eV)
0.4 mmol GeI_2	1.22
0.3 mmol GeI_2	1.05
0.28 mmol GeI_2	1.06

CONCLUSIONS:

Three different sizes of OAM-capped germanium nanoparticles ranging from 4 to 10 nm were synthesized via a microwave method. OAM-capped Ge NPs were subsequently recapped with DDT. Powder x-ray diffraction confirms the presence of diamond cubic Ge in the Ge NP sample. However, there is loss of material during the recapping procedure which resulted in lower concentrations of DDT-capped Ge NPs and lower peak intensities. Bands characteristic to OAM can be seen in the first spectrum, these include the =C-H at 3006 cm^{-1} and the stretching

vibrations of -NH_2 at approximately 3300 cm^{-1}.[20] Both of these bands are not seen in the DDT-capped sample. This indicates that the ligand exchange to DDT was successful.

As the amount of GeI_4 precursor was increased, the size of the Ge NPs also increased. Ge NPs with increasing sizes have been synthesized by other groups by varying the amount of GeI_4.[21, 3] The extinction coefficient changes with Ge NP size, however it is not a linear change with increasing size. This may be due to calculated concentrations of Ge, as it was assumed there was 100% conversion to product during the reaction and that no amount of product was lost during transfer and washing steps. Samples of OAM-capped and DDT-capped Ge NPs were prepared for inductively coupled plasma mass spectroscopy measurements to determine Ge concentration, however there was an error with the sample measurements and Ge concentrations were not able to be collected. Another way determine concentration of Ge is to dissolve and then dry future samples of Ge NPs in order to weigh the Ge in each sample.

CHAPTER 3

Shape Control of Germanium Nanoparticles with Polyvinylpyrrolidone

INTRODUCTION

As the field of nanotechnology progresses, the ability to tune size and shape has become an interesting area of research. Nanoparticles (NPs) of varying shapes have been synthesized, including nanorods, nanoplates, octahedral and tetragonal structures, and more complex shapes like nanostars or nanoflowers.[22] The shape of nanoparticles (NPs) can play a large part in the electronic and optical functionality of the NPs as compared to the bulk material.[23] Applications of NPs in biology, catalytic, and energy-related areas can be tailored from the control of NP shape.

One way in which to control or alter the shape of NPs is by incorporating an additive or surfactant into the synthesis of the NPs. This could be a polymer, halide, amine, or a small molecule. These compounds generally contain a functional group that then becomes the capping agent for the NPs and often multiple additives or surfactants are used in NP synthesis to control shape and growth.[22] Additives can also help to prevent NP aggregation.[24] Depending on the combination of additive/surfactant, metal, and solvent, NP with unique shapes can be synthesized.[24]

Polyvinylpyrrolidone (PVP) is a polymer that has been successfully used in the shape control of metal and semi-metal NPs. PVP contains multiple functional groups and has both a hydrophilic and hydrophobic component.[25] Because PVP is a polymer, chain length is an important factor when PVP is used in NP synthesis, with longer chain lengths being shown to better stabilize Ag NPs.[26] PVP has also been shown to be a shape-directing agent for Ag NPs, attaching preferentially to the Ag (100) plane during NP growth.[24] Au NPs of varying shapes,

such as octahedra and nanostars, have been prepared through PVP-assisted synthesis methods.[25] Chain length and concentration of PVP have also been shown to influence NP shape. PVP molecular weight and concentration resulted in differing shapes of Ag NCs.[26]

In this chapter, experimentation was undertaken to examine the effect of PVP in Ge NP synthesis. The ability to control both the size and shape of NPs has large impacts on the properties and applicability of nanostructures. The goal of this experiment is to investigate the effects of PVP as a shape-control agent in Ge NP synthesis via a microwave method.

EXPERIMENTAL

Methods - Germanium Nanoparticle Synthesis:

All samples were prepared in an Ar-filled glovebox. 0.4 mmol of GeI_2 (purchased from Dr. Richard Blair's laboratory at the University of Central Florida) was added to a 10-mL microwave tube with 4 mL of degassed oleylamine (Sigma-Aldrich, >98%) and 0.02 or 0.01 mmol PVP40. The sample was sealed with a cap inside the glove box and parafilmed three times after being taken out. The PVP did not dissolve in OAM, but the sample was sonicated to dissolve the GeI_2. It was then heated for 30 minutes at 230°C in a CEM microwave reactor. The color of the sample changed to a dark brown during this heating period, indicating the formation of Ge NPs.

Nanoparticle Isolation:

Microwaved samples were triple-wrapped in parafilm and transferred back into the glove box and the contents were transferred into a centrifuge tube. The catalyst tower was closed before isolating the sample in the glove box. Approximately 10 mL of anhydrous ethanol was added and the sample was taken out of the glove box and centrifuged at 8500 RPM for 15

minutes. The centrifuge tube was triple wrapped and transferred back into the glove box. The colorless supernatant was discarded and the nanoparticles on the side of the centrifuge tube. Samples were washed with 10 mL of EtOH and centrifuged for 20 minutes two more times before being suspended in 5 mL of toluene. All samples were stored in glass screw-top vials within the glove box.

Powder X-ray Diffraction (PXRD):

Samples were prepared for PXRD measurements by collecting 0.1 to 0.3 mL of stored sample in a plastic syringe. The syringe was capped and taken out the box. The sample was drop-casted onto a silicon zero-background holder while the holder was heated gently on a hot plate. A Bruker D8 diffractometer (Cu Kα source, λ = 1.5418 Å) was used to collect PXRD data from the 20° to 80° 2θ. The PXRD patterns were compared to diamond cubic Ge (04-0545) diffraction file from the International Center for Diffraction Data.

FT-IR:

Samples of Ge NPs were deposited directly onto crystal on a Bruker Alpha spectrometer. FT-IR measurements were taken after sample was allowed to air dry.

UV-Vis:

1 mL of a capped or recapped sample was taken out of the glove box in a 5-mL glass vial. This sample was then transferred into a quartz cuvette using a micropipette. 2 mL of toluene (Sigma-Aldrich) was dispensed via micropipette to dilute the 1-mL sample of Ge NPs. UV-Vis spectra were collected for serial dilutions of each Ge NP sample. A spectrum of each dilution was collected on a UV-3600 Plus Shimadzu UV-vis-NIR spectrophotometer at room temperature from 1600 to 250 nm. The sampling interval was 1 nm.

Scanning Transmission Electron Microscopy (STEM):

Samples of Ge NPs were prepared for STEM analysis by transferring less than 0.5 mL of stored sample to a separate screw-top vial and taking this vial out of the glove box. The sample was diluted with toluene by a factor of 5:1. A drop of diluted sample was dropped onto a carbon mesh TEM grid that was placed on a paper filter. The grid was left to dry overnight before being placed in a vacuum oven to dry for 24 hours. TEM grids were stored in a holder until taken to by used on a JEOL STEM instrument.

DISCUSSION/RESULTS:

Figure 3-1 shows the PXRD diffraction pattern for Ge NPs synthesized with 0.02 mmol or 0.01 mmol of PVP. The intensity of the peaks is very low in both patterns, with the last two diffraction peaks at 72.9 and 65.2 degrees not appearing at all. The peaks around 38 degrees are from the silicon holder and not from the sample. An FT-IR spectrum of Ge NPs with 0.01 mmol of PVP is shown in Figure 3-2.

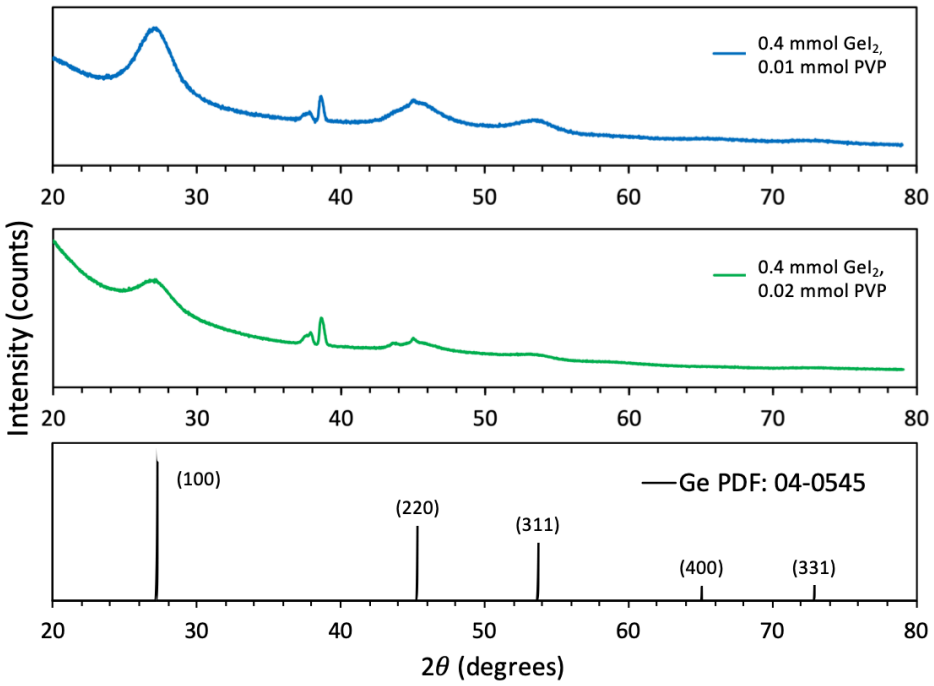

Figure 3-1 PXRD patterns of Ge NPs synthesized with varying amount of PVP40 (0.01-0.02 mmol) compared to Ge reference pattern (Ge PDF: 04-0545).

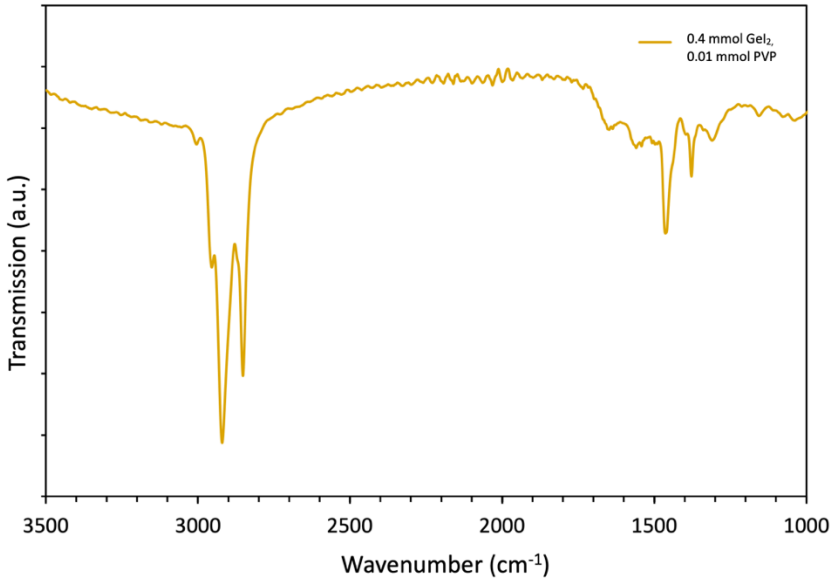

Figure 3-2 FT-IR spectra of Ge NPs synthesized with 0.01 mmol PVP40.

A 0.3 mL sample of diluted sample was taken out of the glove box for absorption measurements. For both Ge NP/PVP samples, 0.2 mL of sample was diluted with 2.80 mL of

toluene for absorption measurements. The spectra for Ge NPs with 0.01 and 0.02 mmol of PVP40 are shown in Figure 3-3.

Figures 3-4 and 3-5 are of both Ge NP/PVP40 samples imaged using STEM. The bright field and dark field micrographs in Figure 3-4 show Ge NPs with 0.02 mmol PVP40 at two separate areas on the sample holder (designated “a” and “b”) and Figure 3-5 is Ge NPs with 0.01 mmol PVP40.

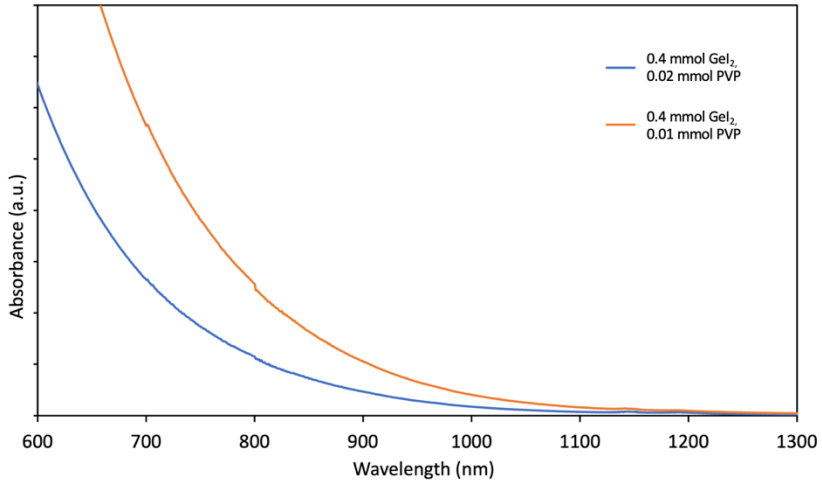

Figure 3-3 UV-Vis-NIR absorbance spectra of Ge NPs synthesized with 0.01 and 0.02 mmol PVP40.

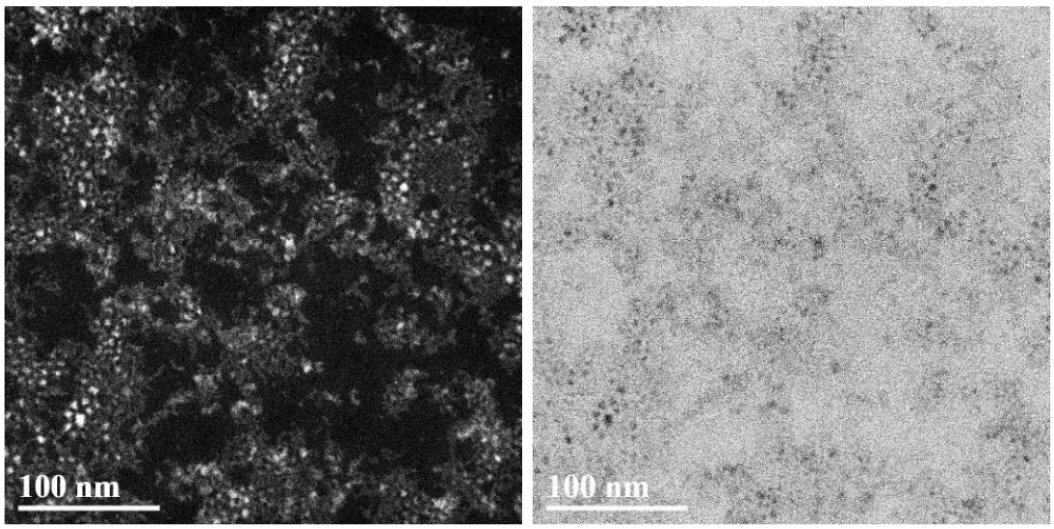

Figure 3-4 Dark field (left) and bright field (left) STEM micrographs of Ge NPs synthesized with 0.01 mmol PVP40.

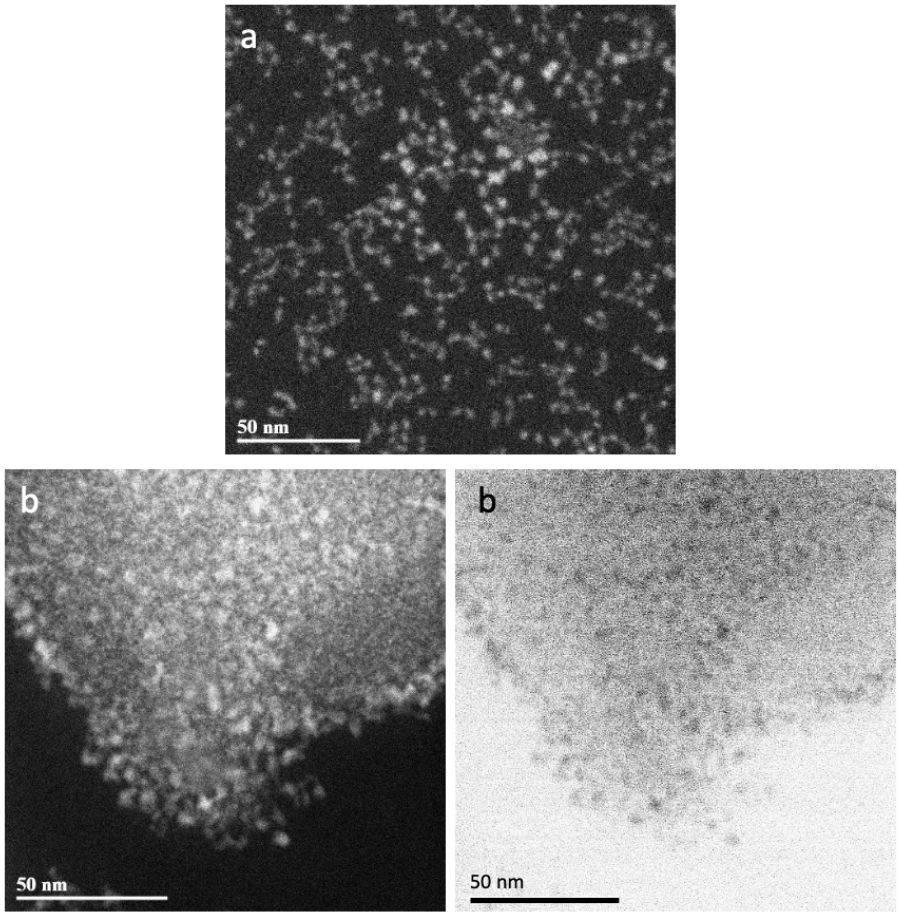

Figure 3-5 STEM micrographs of Ge NPs synthesized with 0.02 mmol of PVP40 at two different areas of sample, area (a) and (b), on same sample holder.

CONCLUSIONS:

Ge NPs were synthesized through microwave synthesis in OAM and with the addition of PVP40. The PXRD patterns of Ge NPs synthesized with 0.01 and 0.02 mmol of PVP (Figure 3-1) show peaks corresponding to the first three (hkl) peaks in the Ge PDF reference pattern. The last two peaks corresponding to the (400) and (331) peaks are not distinguishable from the background in the Ge NP diffraction pattern. The two peaks around 38° are attributed to the silicon sample holder. The low intensity and absence of peaks indicates a low concentration of Ge NPs on the sample holder. The color change from yellow to dark brown after synthesis confirms that nano Ge was produced, however there was most likely some amount of sample lost during NP isolation.

The STEM micrographs in Figure 3-4 show Ge NPs synthesized with 0.01 mmol PVP40. The Ge NPs have no consistent shape, and the sample is overall agglomerated together. The brightest white spots in the dark field micrograph in Figure 3-4 are most likely elemental Ge. Due to the high contrast of these bright spots, this would indicate a higher molar mass of brighter areas imaged using STEM. Both the Ge NPs and Ge NPs are surrounded by substance, possibly remaining PVP40 or polymer. The Ge NPs synthesized with 0.2 mmol PVP40 shown in Figure 3-5 show the same polymer substance in area (b), with some NP being free in other areas of the sample as shown in area (a) of Figure 3-5.

When dissolving the Ge precursor and PVP in OAM, the PVP would often clump onto the GeI_2 making this process time consuming. PVP was found to not be readily soluble in OAM. The sample would need to be sonicated and stirred for longer periods of time compared to Ge NPs synthesized without any PVP added. PVP has been shown to control the shape of semi-metal NP, but polar solvents were used for synthesis.[25,27] As part of this experiment, small

amounts of PVP40 was added to the organic solvent dimethylformamide (DMF) to test solubility. Further research for this project would be to determine whether the addition of a small amount of organic solvent to Ge NP synthesis with PVP40 would aid in dissolving the PVP before the sample is reacted in the microwave. Finding a better system for Ge NP/PVP synthesis would be advantageous for the continuation of this project.

REFERENCES

(1) Xue, D. J.; Wang, J. J.; Wang, Y. Q.; Xin, S.; Guo, Y. G.; Wan, L. J. Facile Synthesis of Germanium Nanocrystals and Their Application in Organic-Inorganic Hybrid Photodetectors. *Adv. Mater.* **2011**, *23* (32), 3704–3707. https://doi.org/10.1002/adma.201101436.

(2) Reiss, P.; Carrière, M.; Lincheneau, C.; Vaure, L.; Tamang, S. Synthesis of Semiconductor Nanocrystals, Focusing on Nontoxic and Earth-Abundant Materials. *Chem. Rev.* **2016**, *116* (18), 10731–10819. https://doi.org/10.1021/acs.chemrev.6b00116.

(3) Vaughn, D. D.; Bondi, J. F.; Schaak, R. E. Colloidal Synthesis of Air-Stable Crystalline Germanium Nanoparticles with Tunable Sizes and Shapes. *Chem. Mater.* **2010**, *22* (22), 6103–6108. https://doi.org/10.1021/cm1015965.

(4) Prabakar, S.; Shiohara, A.; Hanada, S.; Fujioka, K.; Yamamoto, K.; Tilley, R. D. Size Controlled Synthesis of Germanium Nanocrystals by Hydride Reducing Agents and Their Biological Applications. *Chem. Mater.* **2010**, *22* (2), 482–486. https://doi.org/10.1021/cm9030599.

(5) Elayaraja Muthuswamy, Andrew S. Iskandar, Marlene M. Amador, and S. M. K. Facile Synthesis of Germanium Nanoparticles with Size Control: Microwave versus Conventional Heating. **2013**, 1416–1422.

(6) Elayaraja Muthuswamy, Jing Zhao, Katayoun Tabatabaei, Marlene M. Amador, Michael A. Holmes, Frank E. Osterloh, and S. M. K. Thiol-Capped Germanium Nanocrystals: Preparation and Evidence for Quantum Size Effects.

(7) Kerr, A. T.; Placencia, D.; Gay, M. E.; Boercker, J. E.; Soto, D.; Davis, M. H.; Banek, N. A.; Foos, E. E. Sulfur-Capped Germanium Nanocrystals: Facile Inorganic Ligand

Exchange. *J. Phys. Chem. C* **2017**, *121* (41), 22597–22606. https://doi.org/10.1021/acs.jpcc.7b04045.

(8) Vaughn, D. D.; Schaak, R. E. Synthesis, Properties and Applications of Colloidal Germanium and Germanium-Based Nanomaterials. *Chem. Soc. Rev.* **2013**, *42* (7), 2861–2879. https://doi.org/10.1039/c2cs35364d.

(9) Zhu, Y. J.; Chen, F. Microwave-Assisted Preparation of Inorganic Nanostructures in Liquid Phase. *Chem. Rev.* **2014**, *114* (12), 6462–6555. https://doi.org/10.1021/cr400366s.

(10) Gerbec, J. A.; Magana, D.; Washington, A.; Strouse, G. F. Microwave-Enhanced Reaction Rates for Nanoparticle Synthesis. *J. Am. Chem. Soc.* **2005**, *127* (45), 15791–15800. https://doi.org/10.1021/ja052463g.

(11) Dahal, N.; García, S.; Zhou, J.; Humphrey, S. M. Beneficial Effects of Microwave-Assisted Heating versus Conventional Heating in Noble Metal Nanoparticle Synthesis. *ACS Nano* **2012**, *6* (11), 9433–9446. https://doi.org/10.1021/nn3038918.

(12) Pescara, B.; Mazzio, K. A.; Lips, K.; Raoux, S. Crystallinity and Size Control of Colloidal Germanium Nanoparticles from Organogermanium Halide Reagents. *Inorg. Chem.* **2019**, *58* (8), 4802–4811. https://doi.org/10.1021/acs.inorgchem.8b03157.

(13) Xia, C.; Wu, W.; Yu, T.; Xie, X.; Van Oversteeg, C.; Gerritsen, H. C.; De Mello Donega, C. Size-Dependent Band-Gap and Molar Absorption Coefficients of Colloidal CuInS2 Quantum Dots. *ACS Nano* **2018**, *12* (8), 8350–8361. https://doi.org/10.1021/acsnano.8b03641.

(14) Yu, W. W.; Qu, L.; Guo, W.; Peng, X. Experimental Determination of the Extinction Coefficient of CdTe, CdSe and CdS Nanocrystals. *Chem. Mater.* **2004**, *16* (3), 560. https://doi.org/10.1021/cm033007z.

(15) Toufanian, Reyhaneh; Zhong, Xingjian; Kays, Joshua; Saeboe, Alexander; Dennis, A. *ZnSe Quantum Dots: Determination of Molar Extinction Coefficient for UV to Blue Emitters*; **2020**.

(16) Moreels, I.; Lambert, K.; De Muynck, D.; Vanhaecke, F.; Poelman, D.; Martins, J. C.; Allan, G.; Hens, Z. Comment on "Size-Dependent Composition and Molar Extinction Coefficient of PbSe Semiconductor Nanocrystals." *ACS Nano* **2009**, *3* (8), 2053. https://doi.org/10.1021/nn9005363.

(17) Tauc, J.; Grigorovici, R.; Vancu, A. Optical Properties and Electronic Structure of Amorphous Germanium. *Phys. Status Solidi* **1966**, *15* (2), 627–637. https://doi.org/10.1002/pssb.19660150224.

(18) Makuła, P.; Pacia, M.; Macyk, W. How To Correctly Determine the Band Gap Energy of Modified Semiconductor Photocatalysts Based on UV-Vis Spectra. *J. Phys. Chem. Lett.* **2018**, *9* (23), 6814–6817. https://doi.org/10.1021/acs.jpclett.8b02892.

(19) JADE. Materials Data, Inc. 2017.

(20) Mourdikoudis, S.; Liz-Marzán, L. M. Oleylamine in Nanoparticle Synthesis. *Chem. Mater.* **2013**, *25* (9), 1465–1476. https://doi.org/10.1021/cm4000476.

(21) Ruddy, D. A.; Erslev, P. T.; Habas, S. E.; Seabold, J. A.; Neale, N. R. Surface Chemistry Exchange of Alloyed Germanium Nanocrystals: A Pathway toward Conductive Group IV Nanocrystal Films. *J. Phys. Chem. Lett.* **2013**, *4* (3), 416–421. https://doi.org/10.1021/jz3020875.

(22) Wu, Z.; Yang, S.; Wu, W. Shape Control of Inorganic Nanoparticles from Solution. *Nanoscale* **2016**, *8* (3), 1237–1259. https://doi.org/10.1039/c5nr07681a.

(23) Personick, M. L.; Mirkin, C. A. Making Sense of the Mayhem behind Shape Control in

the Synthesis of Gold Nanoparticles. *J. Am. Chem. Soc.* **2013**, *135* (49), 18238–18247. https://doi.org/10.1021/ja408645b.

(24) Qi, X.; Balankura, T.; Zhou, Y.; Fichthorn, K. A. How Structure-Directing Agents Control Nanocrystal Shape: Polyvinylpyrrolidone-Mediated Growth of Ag Nanocubes. *Nano Lett.* **2015**, *15* (11), 7711–7717. https://doi.org/10.1021/acs.nanolett.5b04204.

(25) Koczkur, K. M.; Mourdikoudis, S.; Polavarapu, L.; Skrabalak, S. E. Polyvinylpyrrolidone (PVP) in Nanoparticle Synthesis. *Dalt. Trans.* **2015**, *44* (41), 17883–17905. https://doi.org/10.1039/c5dt02964c.

(26) Xia, X.; Zeng, J.; Oetjen, L. K.; Li, Q.; Xia, Y. Quantitative Analysis of the Role Played by Poly(vinylpyrrolidone) in Seed-Mediated Growth of Ag Nanocrystals. *J. Am. Chem. Soc.* **2012**, *134* (3), 1793-1801. https://doi.org/10.1021/ja210047e.

(27) Kyrychenko, A.; Korsun, O. M.; Gubin, I. I.; Kovalenko, S. M.; Kalugin, O. N. Atomistic Simulations of Coating of Silver Nanoparticles with Poly(Vinylpyrrolidone) Oligomers: Effect of Oligomer Chain Length. *J. Phys. Chem. C* **2015**, *119* (14), 7888–7899. https://doi.org/10.1021/jp510369a.